Journal of Power Sources 268 (2014) 121–128

Contents lists available at ScienceDirect

Journal of Power Sources

journal homepage: www.elsevier.com/locate/jpowsour

Description and performance of a novel aqueous all-copper redox flow battery

Laura Sanz [a, b, *], David Lloyd [a], Eva Magdalena [b], Jesús Palma [b], Kyösti Kontturi [a]

[a] Aalto University, Department of Chemistry, Espoo, Finland
[b] Institute IMDEA Energy, Móstoles, Madrid, Spain

HIGHLIGHTS

- A novel, aqueous chemistry based on copper for use in redox flow cells is presented.
- Comparable energy density to vanadium systems due to high solubility of copper (3 M).
- Uses low cost, less toxic, easily recyclable and abundant materials.
- Simplicity: single step preparation of electrolyte and no catalysts required.
- Elimination of heat exchangers since the operational temperature range is extended.

ARTICLE INFO

Article history:
Received 31 January 2014
Received in revised form
16 May 2014
Accepted 3 June 2014
Available online 12 June 2014

Keywords:
Redox flow batteries
Aqueous electrolytes
Copper-chloride complexes
Cost reduction
Hybrid flow cells

ABSTRACT

In this paper we present a novel aqueous redox flow battery chemistry based on copper chloro complexes. The energy density (20 Wh L^{-1}) achieved is comparable to traditional vanadium redox flow batteries. This is due to the high solubility of copper (3 M), which offsets the relatively low cell potential (0.6 V). The electrolyte is cheap, simple to prepare and easy to recycle since no additives or catalysts are used. The stack used is based on plain graphite electrode materials and a low-cost microporous separator. The system can be operated at 60 °C eliminating the need for a heat exchanger and delivers an energy efficiency of 93, 86 and 74% at 5, 10 and 20 mA cm^{-2} respectively.

1. Introduction

The growing demand for electricity expected during the coming decades has increased interest in the development of new technologies for energy production from renewable power sources, such as wind and solar. However, the success of these new renewable power sources needs to be coupled with the introduction of competitive energy storage devices for load-levelling and peak-shaving such that these renewable sources could be tied to the grid. In this fashion, the problem of the unpredictable and intermittent energy production behaviour of renewable power sources may be overcome. For electrical energy storage, electrochemical devices such as batteries and supercapacitors have been shown to provide higher efficiencies compared to other energy storage systems currently utilized [1,2].

Within the wide variety of electrochemical devices for energy storage, redox flow batteries (RFB) are one of the best options for massive storage due to their higher capacity for massive storage in comparison with other battery technologies. RFBs typically employ two soluble redox couples at high concentrations in aqueous or organic media which are stored in two external tanks and pumped into an electrochemical reactor, where one of the species of the redox couple is transformed into the other, storing or delivering energy depending upon whether the device is charging or discharging. The reactor is composed of a stack of two-electrode cells. The two electrodes are typically composed of graphite bipolar plates and carbon felts. These electrodes are separated by an ionic exchange membrane, typically Nafion, to avoid mixing of the positive and negative half-cell electrolytes [3].

* Corresponding author. Institute IMDEA Energy, Móstoles, Madrid, Spain. Tel.: +34 646369231.
E-mail addresses: laura.sanz@aalto.fi, laurasanzrubio@gmail.com, laura.sanz@imdea.org (L. Sanz), david.lloyd@aalto.fi (D. Lloyd).

http://dx.doi.org/10.1016/j.jpowsour.2014.06.008
0378-7753/

Many types of RFB have been widely explored since the first appearance of the Fe–Cr flow cell in 1973 [4], including hybrid systems and chemically regenerative redox fuel cells [1,2,5–7]. However, only the iron–chromium, all-vanadium (VRB), zinc–bromine and sodium-polysulfide (PSB) have come close to full-scale commercialization. At this point, the reduction of cost of the different materials employed in the electrodes, the membranes and the electrolyte is mandatory to promote the introduction of RFBs in the worldwide market.

A feasible strategy to reduce the cost of RFBs is the total or partial substitution of the half-cell electrolytes of the RFB systems mentioned above by alternative redox couples. These alternative redox couples should be abundant, non-toxic and highly soluble in water. Ideally, they should provide a redox potential close to the anodic and cathodic limits of the operational potential window of the supporting electrolyte, which should be highly conductive and simple to recycle.

In this work, the redox processes of copper species are applied for the first time in an aqueous all-copper RFB, where the three oxidation states of copper are present in a hybrid redox flow configuration. The employment of the same element in both half-cells reduces the problem of cross-contamination across the membrane, allowing the use of simple and cheap microporous separators. All-copper redox batteries have been previously reported based on acetonitrile [8,9] ionic liquids [10] and deep eutectic solvents [11].

1.1. The all-copper system: redox reactions and potential

In previous studies [12], the degree in electrochemical reversibility of the Cu(I)/Cu(II) redox couple in chloride media at 1 M concentration of copper was investigated. It was found that the values of peak potential separations of this couple were comparable to those displayed by vanadium redox couples, showing a quasi-reversible behaviour. In addition, a noticeable displacement of the formal potential of the Cu(I)/Cu(II) redox couple towards much more positive values was observed, reaching the experimental potential displayed by the Fe(III)/Fe(II) redox couple, which has also been widely employed in flow cells, for instance in a hybrid all-iron configuration [13] and more recently in the Fe–V RFB [14–16].

In the all-copper RFB the chemistry of the Cu^0–Cu(I)–Cu(II) system is employed to store and deliver electricity within the battery, as shown in Equations (1) and (2). The fresh electrolyte, which is initially composed by cuprous chloro complexes, is transformed into cupric chloro complexes in the positive half-cell and electrodeposited as copper on the negative electrode surface during charge. Therefore, during discharge, the cupric ions formed in the positive half-cell electrolyte are transformed again to Cu^+ ions, while the stripping of the copper deposit occurs in the negative side.

$$\text{Positive half} - \text{cell reaction}: \quad Cu^+ \underset{\text{Discharge}}{\overset{\text{Charge}}{\rightleftharpoons}} Cu^{2+} + e^- \qquad (1)$$

$$\text{Negative half} - \text{cell reaction}: \quad Cu^+ + e^- \underset{\text{Discharge}}{\overset{\text{Charge}}{\rightleftharpoons}} Cu^0 \qquad (2)$$

The potential difference between these two kinetically facile reactions in highly concentrated chloride media is around 0.7 V according to previous electrochemical studies of copper-chloride electrolytes in aqueous or deep eutectic solvents [11,12].

1.2. Economic and technological potential of the all-copper system

The cell potential of the all-copper system is low compared to RFB chemistries typically used, such as the well-known all-vanadium or Zn–Br systems [1,2,5,6]. However, as this paper will show, the excellent kinetics and the simplicity (no catalyst or ion-exchange membrane required) of the all-copper system coupled with the high concentrations of electroactive species that can be achieved in aqueous media, make this system equally attractive in terms of energy density, energy efficiency and cost per Wh stored. The relatively low power density of the all-copper system is not an insurmountable problem from an economic point of view. The simplicity and the low cost of the materials employed can be expected to offset at least part of the cost of a larger stack. For example, the combined cost of Nafion membranes and vanadium used in a typical all-vanadium RFB is over half the system cost [17]. In the all-copper system the use of simple and cheap nanoporous composite separators, which typically cost 20 to 100 times less than ion exchange membranes [Amersil S.A., personal communication, September 2013] is possible.

Due to the relatively small cell potential the redox processes shown in Equations (1) and (2) are both favoured over the chlorine and hydrogen evolution processes, therefore no gas evolution is likely within this system. This is an important simplification and both eliminates the need for electrolyte balancing mechanisms and safely allows deeper cycling over the entire SOC. Crucially, compared to the dominantly used element, vanadium, copper is abundant, less toxic and can be obtained at extremely high purity at lower cost. Due to the use of three oxidation states preparation of electrolytes is also trivial. In the discharged state the electrolytes in both half-cells are identical and these can be prepared by simply reacting an electrolyte containing any ratio of Cu(II) to Cu(I) with Cu^0. In addition, no catalysts are required since the kinetics of the reactions are impressive on carbon materials. Finally, the heat exchanger of the vanadium system is eliminated since no complications with the stability of the electrolytes was found over a wide range of temperature, from 5 to 70 °C.

The electrolytes can be readily recycled in widespread industrial processes such as electrowinning [18], Hydrocopper® [19] or copper etching [20]. Therefore, the initial investment in the electrolyte can be easily recovered at the end of the life of the battery.

2. Experimental

2.1. Electrolyte preparation

The Cu(I) electrolyte used to fill both storage tanks was prepared from Cu(I) chloride (>99% purity, Acros Organics) salt. The concentration of copper was varied from 1 M up to 3 M in the different cycling tests. In order to increase the concentration of chloride, calcium chloride (>95% purity, Scharlau) and HCl (37% Panreac) were utilized as mixed supporting electrolyte in both half-cells. The respective concentrations of acid and salt were the same in all the solutions; 2 M and 4 M of each in the electrolytes at 1 M and 3 M copper concentration respectively. Cuprous ions are easily oxidized by oxygen so the solutions were stirred with mild heating in contact with metal turnings (Fluka, >99.0%) until they became completely colourless, in order to reduce all the cupric ions that could be formed during the preparation of the electrolytes. However, no further procedures are required in the preparation of the electrolytes.

2.2. Cell assembly

The single flow cell was built using a sandwich type flow reactor (Micro Flow Cell, Electrocell) with graphite electrodes of 10 cm^2 active area in both half-cells. A platinum wire pseudo reference electrode was placed in the positive half-cell in order to record the overpotentials of each electrode separately. Stainless steel and

titanium foils were also tested as electrodes in the negative half-cell, to evaluate their performance as substrates for the electrodeposition of copper. Nanoporous composite separators of PVC-Silica (Amersil S10) were employed. The thickness of the separator was 0.6 mm and the volume of porosity around 70%, with a pore size of 0.08 microns.

2.3. Pumps and storage

The flow rate was controlled by peristaltic pumps (Masterflex L/S Easy Load) and the tubing was made of PVC (Nalgene, 3.6 mm inner diameter), which is particularly suited for use with concentrated HCl.

The hermetically sealed glass electrolyte storage tanks were thermostated using a water bath. Thermometers were inserted inside the tanks to monitor the temperature in the bulk electrolytes. In addition, magnetic stirrers were placed in the tanks to maintain a homogenous mixture of the species. The electrolytes were gently purged with argon before being injected in the tanks. The diffusion of oxygen through the PVC tubing could not be completely avoided during the experiments.

2.4. Cycling tests

Various charge and discharge cycling experiments were performed at constant current after the system had initially been charged from 0 to 50% SOC. The temperature and the flow rates were varied in order to determine the overpotentials of both the charge and discharge processes over a wide range of current densities. The potential was limited up to 0.9 V on charge and down to 0.3 V on discharge.

Charge and discharge experiments at constant current were also carried out to study the stability and the degradation of the process over more than 20 cycles. The flow rate was high enough to ensure good convection of species within the cell compartments (35 mL min^{-1}) while the volume of the electrolytes was 25 mL in each tank. The current density was 20 mA cm^{-2} and the duration of the charge cycles was 1 h, thus the SOC was varied by 10% in each cycle from 50 to 60%.

3. Results

3.1. Initial voltammetric studies

Fig. 1A and B shows the Cu(I)/Cu^0 and Cu(II)/Cu(I) processes respectively at a GC working electrode (5 mm glassy carbon, Pine Research Instrumentation AFE3T050 GC). These were measured using the same electrolyte (3 M CuCl, 4 M HCl/$CaCl_2$) and temperature (60 °C) employed during RFB measurements and were performed sequentially with the same electrolyte and electrode. The reference electrode was a copper wire. To simplify interpretation and make the results as accessible as possible, the electrode was only rotated between each measurement to refresh the solution in front of the electrode and was otherwise stationary.

3.1.1. Negative half-cell reaction

Around 100 mV of overpotential appears to be required for nucleation of copper deposition on GC. Once nucleation occurs, no difference is apparent between the various scan rates used. A slight scan rate dependency during the stripping process can be observed, with a second process apparent at lower scan rates (labelled b in Fig. 1A). This effect has been previously reported by several authors [21,22] and indicates that the stripping of copper in chloride containing solutions proceeds through two stages, an initial process to form an adsorbed CuCl deposit on the copper surface, followed by formation of a $[CuCl_2]^-$ complex [23]. The limiting current density

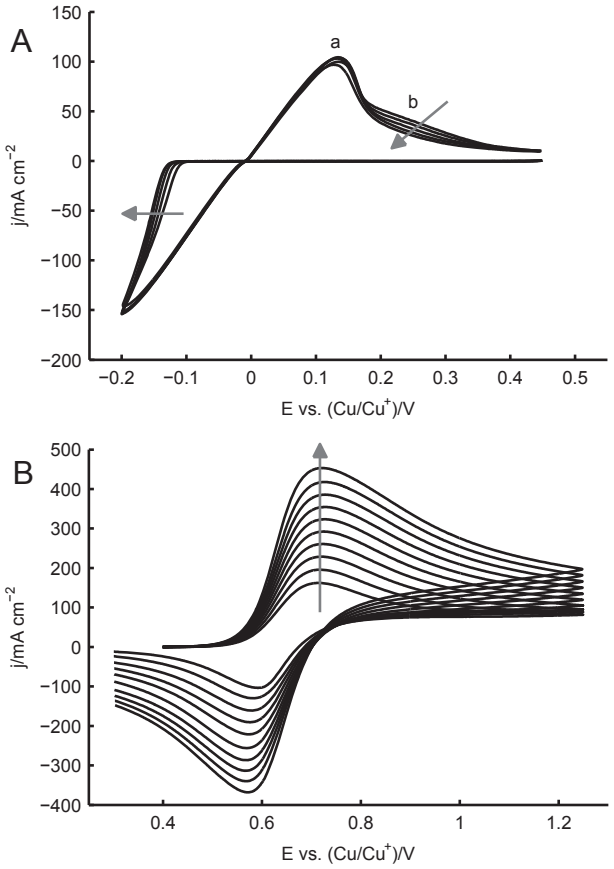

Fig. 1. Cyclic voltammetric measurements for the deposition and stripping of copper (A) and the Cu(I)/Cu(II) reaction in a 3 M Cu(I) solution (B) respectively. The scan rate was varied between 0.2 and 0.02 V s^{-1}. For the sake of clarity only every second scan is shown in Fig. 1A. The arrows indicate the direction of increasing scan rate.

that can be achieved at the negative electrode during discharge is likely related to either transport limitations for free chloride in solution or the kinetics of $CuCl_2^-$ formation. These limitations can be expected to become more pronounced at low temperatures and chloride concentrations [24].

The observed current densities during deposition are favourable, considering that in an actual RFB the intended operating current is around 20 mA cm^{-2}. When the charge passed during deposition and stripping is integrated the Coulombic efficiency is found to be 85 ± 2%, this indicates parasitic losses. By contrast, when the potential is switched at −0.15 V the Coulombic efficiency increases to 94 ± 2%. This dependency of the Coulombic efficiency on the switching potential can most likely be attributed to either hydrogen evolution at excessively negative overpotentials or incomplete stripping of the larger amount of copper deposited at more negative switching potentials.

To further probe the deposition and stripping reactions, the RDE was used to simulate conditions in the negative half-cell of the RFB during operation, using a technique previously reported by Nikiforidis et al. [25]. By rotating the electrode (1000 RPM) a continuous flow of electrolyte passes over the electrode surface, as in an RFB. When a deposition and stripping current density of 20 mA cm^{-2} is applied to an initially uncoated GC electrode a Coulombic efficiency of 90 ± 3% is observed for the first ten cycles (presented in Supplementary data). After this, a drop in the Coulombic efficiency takes place. At the same time the overpotentials required to charge and discharge the cell increases and results in a drop in the voltage efficiency of the deposition and stripping reaction from 94.6 ± 0.9%

to 92.3 ± 0.4%. The open circuit potential measured between the copper reference electrode and GC working electrode after stripping is 34 ± 10 mV and indicates incomplete stripping of the copper deposit. This is also visibly observable, the GC electrode has a matte copper finish at the point when stripping is terminated. Efficient operation of an all-copper RFB over a wide SOC range will require improved understanding and control of the deposition and stripping process.

3.1.2. Positive half-cell reaction

Fig. 1B clearly shows that reaction 1 has facile kinetics. No complicating homogeneous reactions are apparent either. Earlier studies suggest that results measured on GC are indicative for the kinetic behaviour that can be expected on regular graphitic materials [11]. The diffusion coefficient of the Cu(I) complex was determined for each of the anodic peak currents shown in Fig. 1B using the Randles–Sevcik equation and found to be $1.47 \pm 0.03 \times 10^{-6}$ cm^2 s^{-1}. This is an order of magnitude lower than what is commonly reported in aqueous media at ambient conditions and indicates a risk that mass transport limitations will occur at high current densities [26].

The positive half-cell reaction is separated from the chlorine evolution reaction by around 0.8 V, so neither chlorine nor oxygen evolution are expected.

3.2. Influence of the temperature and flow rates over a wide range of current densities

Temperature and flow rate conditions are two of the main parameters affecting the performance of the battery during its operation. Hence, it is important to determine preliminary values of these variables where the battery is able to charge and discharge properly at reasonable efficiencies. As a proof of concept, electrolytes at 1 M concentration of CuCl in 2 M/HCl/$CaCl_2$ were used in these experiments. Short charge and discharge cycles of 10 min were performed after an initial pre-charge to reach a 50% SOC in the electrolytes, varying the flow rate and the current densities at 40 and 60 °C.

The magnitude of the overpotentials on discharge, over a range of current densities from 2 to 60 mA cm^{-2} is plotted in Fig. 2. These overpotentials represent the difference between the OCP of the cell before a charge/discharge step and the potential of the cell during that charge/discharge step. Also the effect of the temperature and flow rate can be observed. These two parameters directly affect the performance of the cell, since the overpotentials are notably decreased when these variables are increased during the operation of the flow battery. At a fixed temperature, the current density that can be applied in the system increases as the flow rate is higher due to an improvement in the convection inside the reactor.

An increase in temperature also allows the use of higher current densities at lower flow rates, which is important to minimize the power consumption of pumps. At 60 °C current densities around 20 or 30 mA cm^{-2} can be easily applied while the overpotentials are not so important at reasonable flow rates.

The overall energy efficiencies displayed in Fig. 3 are close to 100% at low current densities of 2 mA cm^{-2} and independent of the magnitude of the flow rate. However it considerably diminishes with a ten-fold increase in the current density indicating the operational limits of the current configuration of the RFB.

3.3. Effect of temperature on cycling stability tests

The voltage efficiency of the system at 1 M concentration of copper species is around 70% at 40 °C and slightly higher at 60 °C, where 80% can be achieved, as can be shown in Table 1:

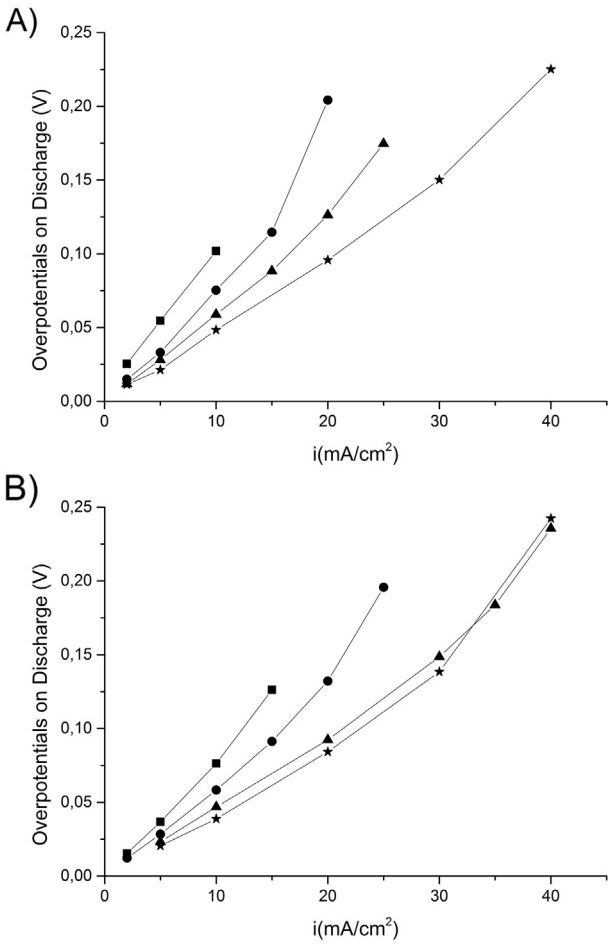

Fig. 2. Overpotentials on discharge of the all-copper RFB; electrodes: graphite; electrolyte: 1 M CuCl/2 M $CaCl_2$/2 M HCl; Separator: Amer-Sil S10; Flow rate: (■) 14 mL min^{-1}; (●) 35 mL min^{-1}; (▲) 70 mL min^{-1}; (★) 140 mL min^{-1}; A) $T = 40$ °C; B) $T = 60$ °C.

The Coulombic efficiency and therefore, the energy efficiency are dramatically affected by the increase in temperature due to cracking of the PVC separator between the gaskets, allowing the crossover of electrolytes. The separator appears to lose some mechanical strength under the mentioned experimental conditions. The area of separator in contact with the electrolytes was not affected during the experiments. An improved reactor design and fibre reinforced gasket materials may reduce the stress on the separator and prevent failure. At 60 °C, the CE drops to 40% in the third cycle, indicating a rapid capacity loss of the system due to the crossover mentioned previously. Therefore the target values of EE and CE are not reached at this temperature. However, at 40 °C the performance of the battery is stable over more than 20 cycles showing CE and EE values around 80% and 60% respectively, as can be observed in Fig. 4.

The operating temperature not only affects the electrochemical performance of the reactions within the cell, but also the structure and morphology of the copper deposits formed on the negative electrode surface, as shown in Fig. 5. At 60 °C, the copper deposits are more compact and homogeneous with a well-defined pentagonal geometry. The size of the grains ranges from 50 to 100 microns approximately, according to the SEM picture in Fig. 5D). At 40 °C, the grains are smaller and their shape is not evident since they tend to form aggregates. The size of these aggregates is around 100 microns, or even higher (Fig. 5C). Therefore, the resulting deposits

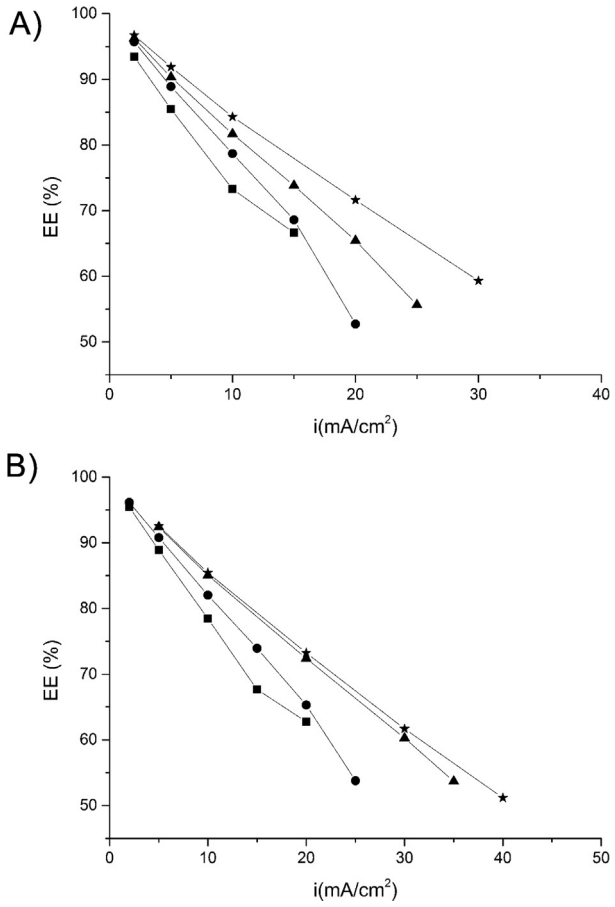

Fig. 3. Influence of temperature and flow rate on the energy efficiencies of the all-copper RFB; electrodes: graphite; electrolyte: 1 M CuCl/2 M $CaCl_2$/2 M HCl; separator: Amer-Sil S10; flow rate: (■) 14 mL min^{-1}; (●) 35 mL min^{-1}; (▲) 70 mL min^{-1}; (★) 140 mL min^{-1}; A) $T = 40$ °C; B) $T = 60$ °C.

are not so compact and homogeneous and it is possible that part of the increase in the overpotentials may also be attributed to a decrease in the conductivity of these deposits in contact with the electrode surface.

3.4. Employment of metallic negative electrodes

One of the strategies to increase the current densities than can be applied in this system is the electrode design and architecture. In these experiments, the negative graphite electrode was replaced by a Stainless Steel (A 316) foil and a Titanium foil (>99.6% purity, Goodfellow) without any pre-treatment. The surface area remains 10 cm^2. The electrolytes were 25 mL of 3 M CuCl/4 M HCl/4 M $CaCl_2$ at 40 °C in each tank. The cycling started at an initial SOC of around 50% (pre-charging) at constant current of 20 mA cm^{-2}.

The CE increases due to an improvement of the electrodeposition and stripping processes over metallic surfaces, as can be observed in Fig. 6.

Table 1
Cell potentials of the all-copper RFB at different temperatures ($i = 10$ mA cm^{-2}; flow rate 35 mL min^{-1}).

Temperature (°C)	Ec (V)	OCV (V)	Ed (V)	VE (%)
40	0.58	0.52	0.42	72
60	0.6	0.54	0.48	80

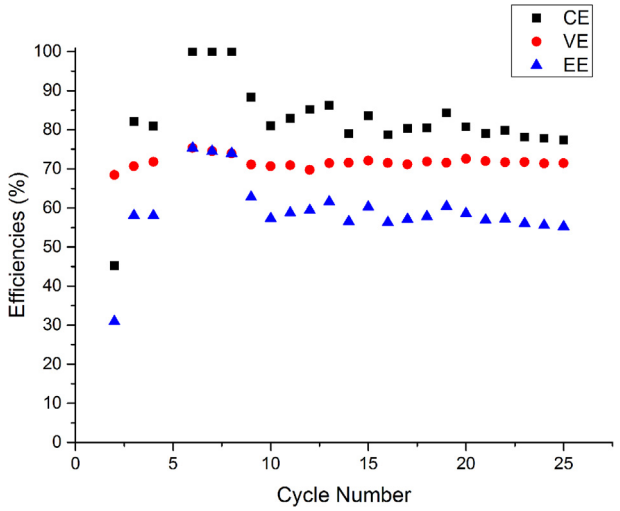

Fig. 4. CE, VE and EE of the all-copper RFB at 40 °C; electrodes: graphite; electrolyte: 1 M CuCl/2 M $CaCl_2$/2 M HCl; separator: Amer-sil S10; flow rate: 35 mL min^{-1}.

The charge profiles are very stable in all the cases. However a slight overpotential in charge is observed when stainless steel is used as the negative electrode. This effect is attributed to parasitic corrosion processes, mainly in the contacts, and is minimized on graphite and titanium electrodes.

In Table 2, the CE, VE and EE of the three systems are calculated from average values of potential and duration of the charge and discharge cycles and they are compared under the same experimental conditions of temperature, flow rate and current density. The CE clearly improves when metallic electrodes are used, as mentioned before. However, the VE is quite similar in all cases and hence, the overall EE is improved with metallic electrodes due to the higher values of CE.

Therefore, the employment of metallic substrates seems to be favourable for the copper electrodeposition process, especially when chemically resistant metals such as titanium are used. However, the performance of ordinary stainless steel is very close to that exhibited by titanium electrodes, although corrosion problems can be anticipated in the presence of highly concentrated chloride media. The efficiencies of charge and discharge cycles of the all-copper RFB at 3 M concentration of copper species are displayed in Fig. 7. At 20 mA cm^{-2} the efficiencies are quite stable over almost 50 cycles and then start to decrease to values of 83% CE, 47% VE and 40% EE.

The low efficiencies are not only attributable to inefficiencies in the chemistry of the system over the long cycling process. Also, the simple design of the reactor, the connections, the diffusion of oxygen through the PVC pipelines and the observable crossover through the separator, limit the efficiencies than can be achieved at a given current density.

Microscope and SEM images of the deposit of copper formed on the surface of the stainless steel electrode after the experiment are shown in Fig. 8. The grains are significantly smaller (10–20 microns) than the ones formed on the surface of graphite electrodes and the layer is much more compact. The structure and geometry of the grains are well defined. The morphology of copper deposits directly affects the electrochemical activity [27] and more importantly, the corrosion behaviour of this metal in presence of chloride ions. The grain size reduction result in improved physical and mechanical properties such as intergranular corrosion and stress corrosion cracking (SCC) [28], [29]. Therefore, the improvement in CE of the flow cell when metallic substrates are used can be

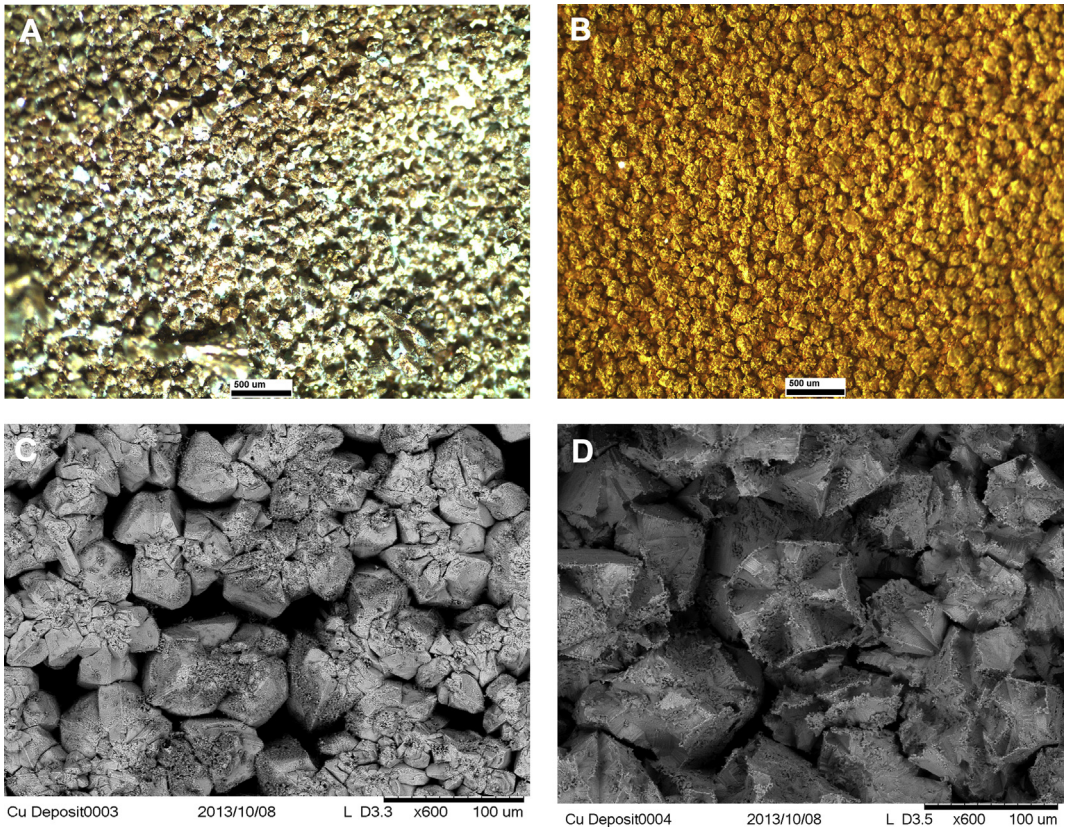

Fig. 5. Optical microscope images (×30); A) $T = 40$ °C; B) $T = 60$ °C and SEM (×600) images of copper deposits formed on graphite electrodes; C) $T = 40$ °C; D) $T = 60$ °C; $i = 10$ mA cm^{-2}.

also attributed to a higher stability of the copper deposits due to their structure and smaller grain sizes.

In addition, a compact layer of salt can be clearly observed on the surface of the copper deposit. The presence of CuCl precipitate is confirmed by EDX analysis in accordance to the voltammetric responses discussed previously, indicating that the stripping process of the copper deposits formed during charge is not as simple as the electrodeposition and combines various steps, involving CuCl intermediates in the mechanism.

Table 2
Comparison of CE, VE and EE of the all-copper RFB using different negative electrodes. The current density was 20 mA cm^{-2} and the temperature was 40 °C.

System ($T = 40$ °C)	i (mA cm^{-2})	CE (%)	VE (%)	EE (%)
3 M graph–graph	20	70	60	42
3 M graph–SS	20	88	57	47
3 M graph–Ti	20	90	58	50

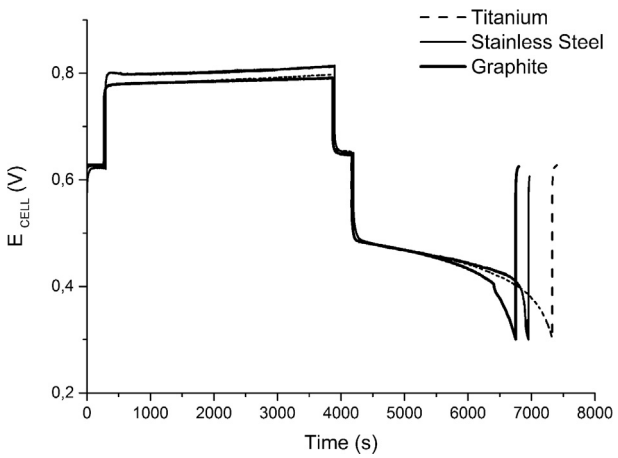

Fig. 6. Comparison of charge/discharge cycles of the all-copper RFB at [Cu] = 3 M; [$CaCl_2$] = 4 M; [HCl] = 4 M; $T = 40$ °C; $i = 20$ mA cm^{-2}; FR = 35 mL min^{-1}.

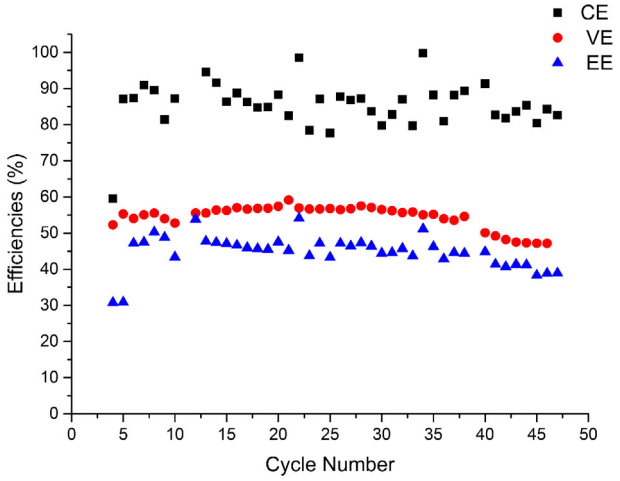

Fig. 7. Cycling stability test of the all-copper RFB with stainless steel negative electrodes; [Cu] = 3 M; [$CaCl_2$] = 4 M; [HCl] = 4 M; $T = 40$ °C; $i = 20$ mA cm^{-2}; FR = 35 mL min^{-1}.

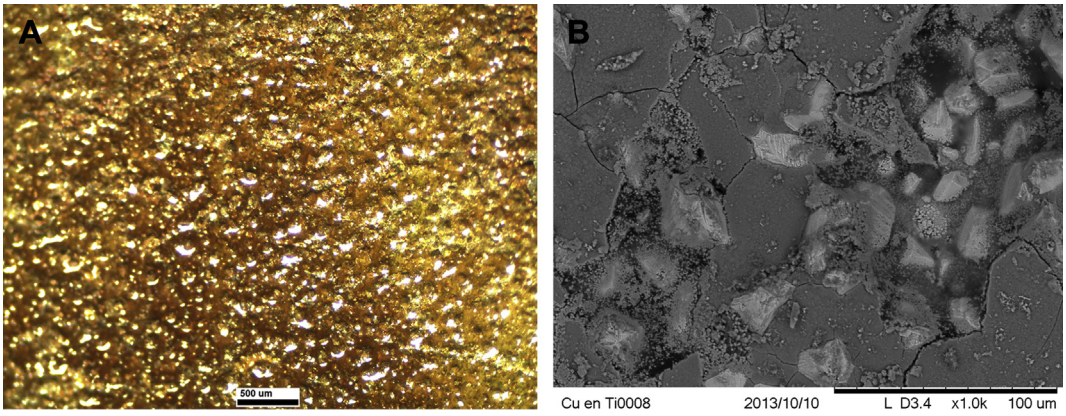

Fig. 8. A) Optical microscope (×30) images and B) SEM (×1000) images of the copper deposit formed on the surface of stainless steel negative electrode after the cycling stability test; $i = 20$ mA cm^{-2}; $T = 40$ °C.

4. Conclusions

The cell used was a general purpose commercial electrochemical device and not optimized for RFB experimentation. The large electrode separation of 8 mm results in significant ohmic losses and these will account for three quarters of the overpotential observed at current densities typically used in RFBs. The performance data presented is therefore of a preliminary nature. However, the results obtained clearly validate the concept of an aqueous all-copper system and establish indicative values for the operational parameters.

The novel electrochemistry of the all-copper system appears well suited to application in RFB technologies. Copper is produced in a highly pure form at a scale of tens of millions of tonnes per year, is less toxic and significantly cheaper than many other materials widely used in RFB systems. The excellent kinetics of redox processes involving copper chloro-complexes, coupled with the high concentrations that can be achieved in aqueous media balance the low cell potential when compared to commercial systems such as the all-vanadium or the hybrid Zn–Br RFB and make this system competitive from the point of view of energy density. Favourable reaction kinetics also eliminate the need for catalysts and reduces the risk of gas evolution during charging of the battery. In this regard the all-copper system compares favourably with the only other hybrid RFB based on a single element, namely the all-Iron battery [13], where energy efficiencies no higher than 55% were reported and significant hydrogen evolution was observed.

The elimination of the catalyst allows a substantial decrease in system cost and should result in fewer complications during the operational lifetime of the battery. Another important cost reduction comes from the use of nanoporous composite PVC/Silica separators instead of ion exchange membranes, especially compared to those based on Nafion® materials. Since the same element is present in both half-cells and only three redox states are involved, cross contamination problems are minimized and in case it occurs, the electrolytes can be easily regenerated using the same single-step comproportionation reaction reported in the experimental section. Cross-contamination problems through the nanoporous separators are not completely avoided at this point; however this problem may be considerably minimized by optimizing the pore size and separator thickness.

The operating temperature can be increased to 60 °C once the damage to the separator caused by mechanical stresses resulting from movement of the gasket materials during compression are eliminated, this would extend the temperature range of operation beyond that of the all-vanadium system, eliminating the need for heat-exchangers. High energy efficiencies (90%) are obtained at low current densities of around 5 mA cm^{-2} and may be also reproducible at higher current densities for an optimized stack design.

Metallic negative electrodes show an improved performance compared to graphite electrodes in terms of Coulombic efficiency. The copper deposited on metallic electrodes appears to be more stable and the grains are smaller and well defined, this favours the stripping process on discharge.

Acknowledgements

The authors wish to thank the MIDE program at Aalto University and the Institute Imdea Energy for their financial support.

Appendix A. Supplementary data

Supplementary data related to this article can be found at http://dx.doi.org/10.1016/j.jpowsour.2014.06.008.

References

[1] M. Skyllas-Kazacos, M.H. Chakrabarti, S.A. Hajimolana, F.S. Mjalli, M. Saleem, J. Electrochem. Soc. 158 (2011) 55–79.
[2] P. Alotto, M. Guarnieri, F. Moro, Renewable Sustainable Energy Rev. 29 (2014) 325–335.
[3] A. Parasuraman, T.M. Lim, C. Menictas, M. Skyllas-Kazacos, Electrochim. Acta 101 (2013) 27–40.
[4] M. Bartolozzi, J. Power Sources 27 (1989) 219–234.
[5] C. Ponce de León, A. Frías-Ferrer, J. González-García, D.A. Szánto, F.C. Walsh, J. Power Sources 160 (2006) 716–732.
[6] A.Z. Weber, M.M. Mench, J.P. Meyers, P.N. Ross, J.T. Gostick, Q. Liu, J. Appl. Electrochem. 41 (2011) 1137–1164.
[7] W. Wang, Q. Luo, B. Li, X. Wei, L. Li, Z. Yang, Adv. Funct. Mater. 23 (2012) 970–986.
[8] B. Kratochvil, K.R. Betty, J. Electrochem. Soc. 121 (1974) 851–854.
[9] P. Peljo, D. Lloyd, N. Doan, M. Majaneva, K. Kontturi, Phys. Chem. Chem. Phys. 16 (2014) 2831–2835.
[10] W.W. Porterfield, J.T. Yoke, Inorganic Compounds with Unusual Properties, ACS Publications, Washington, DC, 1976, p. 104.
[11] D. Lloyd, T. Vainikka, K. Kontturi, Electrochim. Acta 100 (2013) 18–23.
[12] L. Sanz, J. Palma, E. García, M. Anderson, J. Power Sources 224 (2013) 278–284.
[13] L.W. Hruska, R.F. Savinell, J. Electrochem. Soc. 128 (1981) 18–25.
[14] W. Wang, S. Kim, B. Chen, Z. Nie, J. Zhang, G. Xia, L. Li, Z. Yang, Energy Environ. Sci. 4 (2011) 4068–4073.
[15] W. Wang, L. Li, Z. Nie, B. Chen, Q. Luo, Y. Shao, X. Wei, F. Chen, G. Xia, Z. Yang, J. Power Sources 216 (2012) 99–103.
[16] B. Li, L. Li, W. Wang, B. Chen, X. Wei, Q. Luo, Z. Yang, V. Sprenkle, J. Power Sources 229 (2013) 1–5.
[17] V. Viswanathan, A. Crawford, D. Stephenson, S. Kim, V. Sprenkle, J. Power Sources 247 (2014) 1040–1051.
[18] M. Lundström, K. Aromaa, O. Forsén, O. Hyvärinen, M. Barker, Hydrometallurgy 77 (2005) 89–95.
[19] M. Lundström, K. Aromaa, O. Forsén, Hydrometallurgy 95 (2009) 285–289.

[20] O. Cakir, J. Mater. Process. Technol. 175 (2006) 63–68.
[21] D. Starosvetsky, O. Khaselev, M. Auinat, Y. Ein-Eli, Electrochim. Acta 51 (2006) 5660–5668.
[22] S. Kologo, M. Eyraud, L. Bonou, F. Vacandio, Y. Massiani, Electrochim. Acta 52 (2007) 3105–3113.
[23] K. Shi, K. Hu, S. Wang, C. Lau, K. Shiu, Electrochim. Acta 52 (2007) 5907–5913.
[24] H. Zhao, J. Chang, A. Boika, A.J. Bard, Anal. Chem. 85 (2013) 7696–7703.
[25] G. Nikiforidis, L. Berlouis, D. Hall, D. Hodgson, J. Power Sources 206 (2012) 497–503.
[26] P. Kiekens, R.M.H. Verbeeck, E. Temmerman, Microchim. Acta 2 (1981) 29–36.
[27] E. Martinez-Lombardia, Y. Gonzalez-Garcia, L. Lapeire, I. De Graeve, K. Verbeken, L. Kestens, J.M.C. Mol, H. Terryn, Electrochim. Acta 116 (2014) 89–96.
[28] S.H. Kim, K.T. Aust, F. Gonzalez, G. Palumbo, Plat. Surf. Finish. 91 (2004) 68–70.
[29] W. Deng, P. Lin, Q. Li, G. Mo, Corros. Sci. 74 (2013) 44–49.